Published by Avanti Publishers

Global Journal of Energy Technology Research Updates

ISSN (online): 2409-5818

Thermo-Economic Performance of Organic Rankine Cycle-Based Waste Heat Recovery for Power Generation at a Wide Range of Operating Conditions

Gerutu B. Gerutu[1], Ramadhani O. Kivugo[1], Frank Lujaji[1] and Pius V. Chombo[2,*]

[1]*Department of Mechanical Engineering,* [2]*Department of Electrical Engineering, Dar es Salaam Institute of Technology, P.O. Box 2958, Dar es Salaam, Tanzania*

ARTICLE INFO

Article Type: Research Article

Keywords:
RORC
BORC
Organic rankine cycle
Economic assessment
Technical performance

Timeline:
Received: July 04, 2023
Accepted: October 14, 2023
Published: November 14, 2023

Citation: Gerutu GB, Kivugo RO, Lujaji F, Chombo PV. Thermo-economic performance of organic rankine cycle-based waste heat recovery for power generation at a wide range of operating conditions. Glob J Energ Technol Res Updat. 2023; 10: 1-23.

DOI: https://doi.org/10.15377/2409-5818.2023.10.1

ABSTRACT

This study assesses the performance of organic Rankine cycle-based waste heat recovery systems under different working fluids and operating conditions. The basic ORC (BORC) and ORC with recuperator (RORC) are investigated for power generation and economy using toluene and benzene. Thermodynamic and economic indicators are studied at various expander inlet temperatures, expander inlet pressure, evaporation temperature, and condensation temperature. RORC achieves higher ηth by reducing heat source in the evaporator whereas BORC recovers more waste heat and improves Pnet. With toluene, BORC improves Pnet when increasing the expander inlet temperature and pressure. The lowest LCOE of 0.0532 US$/kWh is from BORC operated with toluene at a Pnet of 349 kW and decreases with an increase in expander inlet temperature. The addition of a recuperator adds to the costs of initial investment and LCOE and slightly improves the performance of the ORCs for waste heat recovery.

*Corresponding Author
Email: piusvictor2013@gmail.com
Tel: +(255) 743 453938

1. Introduction

The fossil energy crisis and environmental concerns have emerged as serious issues in recent decades as a result of increased global energy demand [1-5]. As the world's population grows, so does the demand for energy in power generation and industry. Unfortunately, increased energy demand has resulted in the use of fossil fuels, which has a negative impact on the environment. Aside from endangering the environment, a large portion of waste heat generated during power generation is left unused [6] and discharged into the surrounding environment, resulting in significant heat loss accounting for up to 50% of the fuel energy [7, 8]. To that end, reusing waste heat as a useful energy source has the potential to save fuel and reduce emissions. So far, waste heat recovery based on the organic Rankine cycle (ORC) has primarily been used to recover discarded thermal energy from power plants to save fuel, reduce emissions, and significantly increase power production.

The suitability [9] and high efficiency [10, 11] of the ORC have made it an attractive technology [11] for converting waste heat into useful energy. Nevertheless, the variations in the field working conditions are prone to lower the performance of the ORC and cause failure subsequently. For instance, the ORC thermal efficiency is reported to be less than 12%, which hinders commercial adoption [12, 13]. To date, the focus of many researchers is on assessing the performance of ORC configurations [14-16] under variations of heat source [17-19], working fluids [20-22], strategy control, and part-load [23-25], operational parameters [26, 27]. Song *et al*. [9] investigated the performance of a 534 kW basic ORC that used six working fluids to generate power from the gas turbine's flue gas. Their analysis revealed that varying the inlet temperatures of the heat source and the cooling medium has a significant impact on the ORC system's mass flow rate, net power output, and heat utilization ratio. Jinglu *et al*. [28] studied the performance of basic ORC (BORC) using R245fa as a working fluid for geothermal applications. The effects of heat source, condensation, evaporation, superheating, and super-cooling temperatures were considered. Pierobon *et al*. [29] used a recuperated ORC (RORC) to recover waste heat from the SGT 500 gas turbine exhaust with temperature ranges of 350–400 °C by varying the heat source and working fluid. Chacartegui *et al*. [30] examine the performance of BORC for waste heat recovery from seven commercial gas turbines operated by employing R-113, R-245, isobutene, toluene, cyclohexane, and isopentane at different expander inlet temperatures. The results showed that varying the expander inlet temperature with toluene and cyclohexane improved performance and contributed to a thermal efficiency of up to 60% in the combined cycle. Liu *et al*. [31] investigated the power generation performance of an intercooler gas turbine linked to a BORC using n-butane (R600), n-pentane (R601), toluene, and n-heptane while varying the ambient temperature and heat source. When operated with toluene, their analysis revealed a maximum improvement in net power output and thermal efficiency of 6.08 % and 2.14 %, respectively. Algieri and Morrone [32] conducted a parametric analysis of BORC with an internal heat exchanger operated with cyclohexane, decane, and toluene. At the ORC's expander inlet, the effects of system saturation and superheated conditions were investigated. Ventura and Rowlands [33] explored the performance of RORC with various working fluids at heat sources of 100 and 250 °C and expander inlet pressure of up to 6.1 MPa. Despite the improvement of power production with RORC, there was a threshold expander inlet pressure above which the recuperator could not have a positive impact on the power production of all working fluids. In the preceding studies, a single type of ORC was thoroughly studied. According to Rahbar *et al*. [34], BORC and regenerative ORCs are the most studied for application in low heat sources and limited operating conditions. However, to better understand operational performance under varying operating conditions, it is useful to compare different ORC configurations under similar environmental conditions and examine their thermodynamic performances. Reis *et al*. [35] compared the performance of BORC and regenerative ORC operated with toluene for waste heat recovery at various heat sources and discovered that BORC is capable of heat recovery and contributed approximately 20.3 % of the electricity generated. Valencia *et al*. [36] compared the thermodynamic performance of BORC, double-pressure, and RORC with cyclohexane, toluene, and acetone under the influence of evaporating pressure. Fontalvo *et al*. [37] compared the waste heat recovery capabilities of BORC, RORC, and dual-pressure ORC when using R1234yf, R1234ze (E), and R1234ze (Z) and heat sources ranging from 100 to 200 °C. Rashwan *et al*. [38] investigated the thermodynamic performance of BORC, RORC, and cascaded closed loop cycles using propane as the working fluid by varying the expander inlet temperature, expander inlet pressure, condensation temperature, and mass flow rate. As mentioned above, most ORC performance comparisons have been conducted using lower heat sources [34]and under limited operating conditions. As a

result, different ORC configurations are not fully understood from a technical [9] and economic [8, 39] point of view. Apart from improving thermal efficiency, RORC has rarely been compared to other configurations, particularly for recovering high heat sources. In this light, the thermodynamic and economic performance of BORC and RORC for gas turbine waste heat recovery at variable heat sources and operating conditions must be thoroughly compared.

The purpose of this study is to better understand the thermodynamic and economic performance of BORC and RORC coupled with gas turbines while using toluene and benzene as working fluids and utilizing high-temperature heat sources (280 and 500°C). The study is carried out by varying the expander inlet temperature and pressure, as well as the condensation and evaporation temperatures. The effect of operating conditions on BORC and RORC thermodynamic and economic performance is investigated. Thermodynamic indicators such as net power output (P_{net}) and thermal efficiency (η_{th}), as well as economic indicators such as net present value (NPV), rate of return (ROR), and levelized cost of electricity (LCOE), are assessed.

2. Methodology

2.1. System Description

This study uses two cycle configurations, basic ORC (BORC) and recuperated ORC (RORC). Fig. (**1a-b**) depicts the schematic diagrams of the above ORCs. The BORC (Fig. **1a**) comprises of an evaporator (Eva_1), turbine, condenser, and pump. At first, the waste heat is exploited from the natural gas-fueled gas turbine and delivered to the Eva_1. The working is then pressurized to the heat exchanger (HEX_1) with pump (P_1) to gain the heat energy, producing elevated temperature and pressurized fluid. The pressurized fluid expands through the expander (Eva_1) to perform mechanical work which then spins the generator to generate electrical energy. The discharged fluid from the expander (Exp_1) is condensed to liquid in the condenser (C_1), and the second cycle starts.

The schematic of RORC configuration is shown in Fig. (**1b**), similar to BORC except that it contains a recuperator to preheat the fluid before entering the evaporator (Eva_2). The fluid is first pressurized by the pump (P_2) for simplifying the analysis, cycle 1 (ORC 2) receives the heat at first, and the pump pressurizes the working fluid to a specified pressure (state 6-7 and state 7-8). Next, the pressurized working fluid first absorbs the heat from the recuperator then enters to evaporator and converts to a saturated vapor (state 9-1). The saturated vapor from the evaporator, quality = 1, expands in the expander to perform work and produce mechanical power, then generate electricity (state 1-2). After executing the work in the expander (Exp_2), finally, the saturated vapor leaves the expander (Exp_2) and enters to recuperator (state 3-4) before entering the condenser for condensation, water is used as cooling media in the condenser to reject the heat (state 5-6), quality = 0, before entering the pump (P_2) to complete the cycle.

The thermodynamic states of the BORC and RORC configuration cycles are depicted in Fig. (**1c**) and (**1d**), respectively. The diagrams depict the temperature-specific entropy (T-s) of the two configuration cycles. The critical information about the state points (numbers on colored regions), the heat source (red line), and the cooling medium (blue line) is shown in Fig. (**1c**) and (**1d**).

2.2. Mathematical Modeling

Several assumptions have been made to simplify the modeling of two ORC configuration cycles to keep this study simple. The assumptions used are listed below. The assumed parameters and boundary conditions are given in Table **1**.

i. The cycles are considered to reach steady-state conditions
ii. The potential and kinetic energy are neglected
iii. The fluid in the inlet of the pump is a saturated liquid
iv. The friction, heat losses, and pressure drop within the cycle are negligible

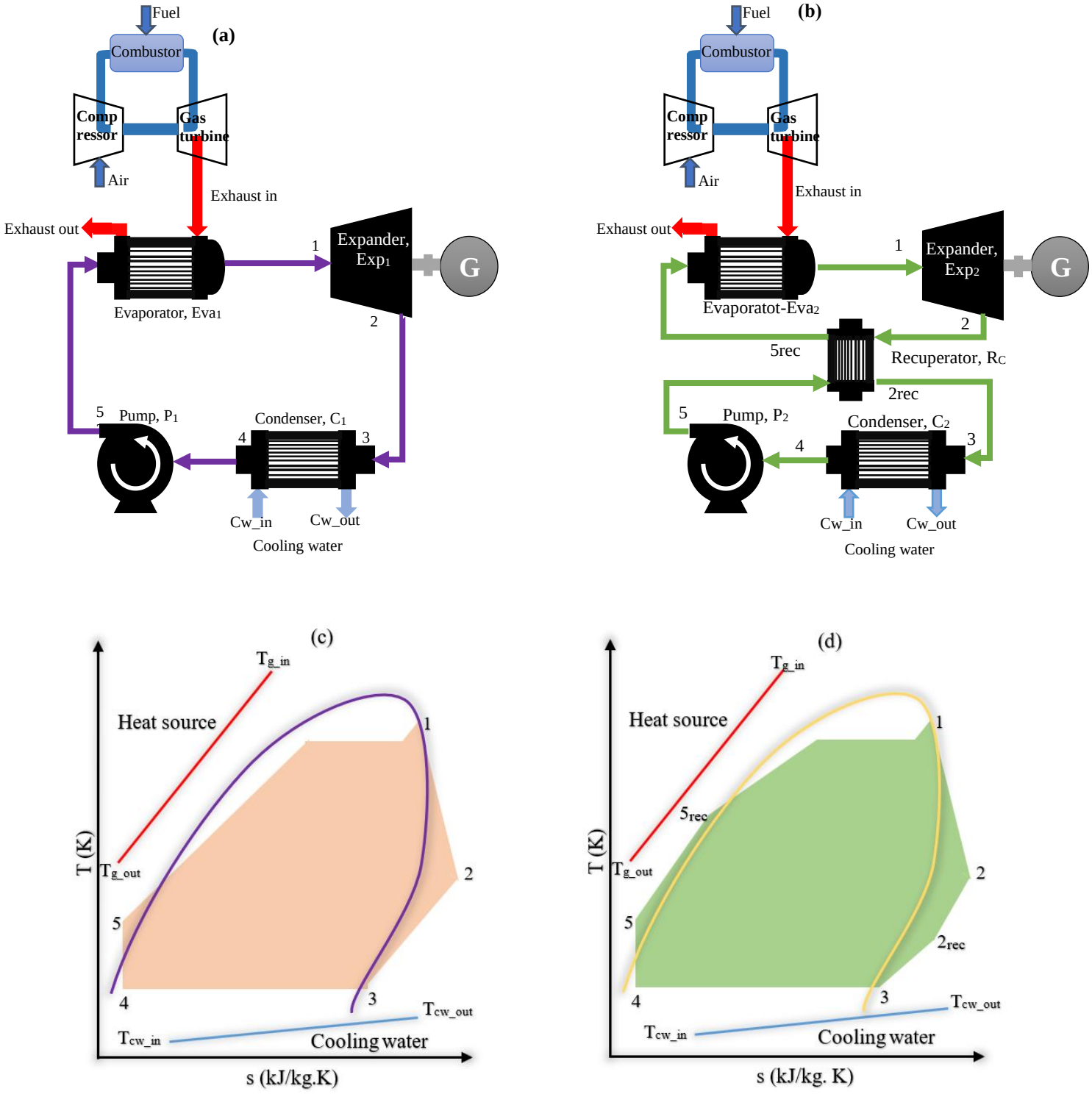

Figure 1: Schematic diagram of (**a**) BORC and (**b**) RORC. T-s diagram of (**c**) BORC and (**d**) RORC.

2.2.1. BORC Cycle Modeling

The BORC cycle primarily consists of an evaporator (Eva_1), expander (Exp_1), condenser (C_1), and pump (P_1). Based on the conversation of mass and energy balance, mathematical modeling for each BORC component can be computed.

Table 1: Boundary condition for simulation.

Parameter	Symbol	Unit	Value	Ref.
Turbine efficiency	η_t	%	0.85	[11]
Evaporator efficiency	η_e	%	0.85	[11]
Condensation efficiency	η_c	%	0.85	[11]
Pump efficiency	η_p	%	0.70	-
Generator efficiency	η_g	%	0.95	-
Evaporation temperature	$T_{\_eva}$	K	783	-
Condenser temperature	$T_{\_cond}$	K	303	-
Cooling inlet water temperature	$T_{\_water}$	K	288	Assumed
Ambient temperature	$T_{\_amb}$	K	298	Assumed
Ambient pressure	P_{amb}	kPa	13690	Assumed
Pinch point temperature difference	*PPTD*	K	8	Assumed

In the evaporator, the total heat energy extracted from the exhaust is given by Eqn. (1).

$$Q_{eva1} = \dot{m}_{wf}(h_1 - h_5) = \dot{m}_{ext,g}(h_{eva1,in} - h_{eva1,out}) \tag{1}$$

where Q and Eva_1 stand for heat gain from the exhaust gas to the working fluid and evaporator of BORC, respectively. m, 1, and 5 stand for the mass flow rate of the working fluid, outlet, and inlet of the evaporator. The subscripts wf, ext, g, ext, in and ext, out stand for working fluid, exhaust gas, exhaust gas at the inlet of the evaporator, and exhaust gas at the outlet of the evaporator.

The work output of the turbine is calculated by using Eqn. (2).

$$W_{Exp1} = \dot{m}_{wf}(h_1 - h_2) = \dot{m}_{wf}(h_1 - h_{2s}) \times \eta_{Exp1} \tag{2}$$

where *W and* Exp_1 stand for work output and expander of BORC, respectively. 1, 2, and 2s stand for enthalpy expander inlet, enthalpy turbine outlet, and expander outlet isentropic condition.

The heat rejected by the condenser is given by using Eqn. (3).

$$Q_{C1} = \dot{m}_{wf}(h_3 - h_4) = \dot{m}_{cw}(h_{cw,out} - h_{cw,in}) \tag{3}$$

where $\dot{Q}$ and C_1 stand for heat removed by the condenser and condenser of BORC. The subscripts w, cw, in, and cw, out means the cooling water, cooling water at the inlet of the condenser, and outlet of the condenser.

The work done by the pump is given by using Eqn. (4).

$$W_{P1} = \dot{m}_{wf}(h_5 - h_4) = \dot{m}_{wf}(h_{5s} - h_4) \Big/ \eta_{P1} \tag{4}$$

where W*P1 and* P1 stand for work of the pump and pump of BORC respectively.

Net power output of the BORC is computed by using Eqn. (5)

$$W_{net} = W_{Exp1} - W_{P1} \tag{5}$$

Thermal efficiency of BORC

$$\eta_{th} = \frac{W_{net}}{\dot{Q}_{eva1}} \times 100\% \tag{6}$$

where W represents the work, the subscripts net and mean net, and thermal η_{th}, respectively.

2.2.2. RORC Cycle Modeling

The RORC cycle comprises of evaporator (Eva_2), expander (E_2), recuperator (R_2), condenser (C_2), and pump (P_2). The mathematical modeling for each RORC component is given below.

Heat gained by the working fluid in the evaporator of RORC (Eva_2)

$$Q_{eva2} = \dot{m}_{wf}(h_1 - h_{5rec}) = \dot{m}_{ext,g}(h_{eva2,in} - h_{eva2,out}) \tag{7}$$

The work done by the turbine (T_2)

$$W_{Exp2} = \dot{m}_{wf}(h_1 - h_2) = \dot{m}_{wf}(h_1 - h_{2s}) \times \eta_{Exp2} \tag{8}$$

Heat added in the recuperator (R_2)

$$Q_{rec2} = \dot{m}_{wf}(h_{5rec} - h_5) \tag{9}$$

where the subscript R_2 stands for recuperator.

The heat rejected by the condenser 2 (C_2) is given by

$$Q_{C2} = \dot{m}_{wf}(h_{2rec} - h_4) \tag{10}$$

where the subscript C_2 means condenser for the RORC.

Work done by the pump 2 is expressed as

$$W_{P2} = \dot{m}_{wf}(h_5 - h_4)/\eta_{P2} \tag{11}$$

Net power output of the RORC is computed as

$$W_{net} = W_{Exp2} - W_{P2} \tag{12}$$

Thermal efficiency

$$\eta_{th} = \frac{W_{net}}{\dot{Q}_{eva2}} \times 100\% \tag{13}$$

2.3. Working Fluid Selection

The choice of the cycle working fluid is a critical stage for the optimal cycle configuration, aiming to match the energy requirement. Moreover, the peer selection process of the working fluids requires bearing in mind several factors such as heat source temperature, safety, fluid stability, environmentally benign, non-flammability, non-toxicity, low viscosity, and cost. In this section, the level of heat source from the gas turbine recovered accounts for fluid section criteria. The list of the commonly used working fluids from the previous studies that have been

adopted in this study is shown in Table **2**. The fluid candidates are benzene and toluene, chosen due to their high critical temperatures below the heat-source temperature. All thermodynamic properties for the selected fluid are retrieved from the CoolProp database.

Table 2: Thermodynamic properties of the working fluid [11, 40].

Fluid Name	Chemical Formula	Molar Mass	Critical Temperature	Critical Pressure	Boiling Point	ODP	GWP
		(g/mol)	(°C)	(Pa)	(°C)	(-)	(-)
Benzene	C_6H_6	78.11	288.9	4.894	80.17	0	low
Toluene	C_7H_8	92.14	318.6	4.126	110.6	0	low

2.4. Economic Modeling

The economic assessment of ORC's system investment includes both direct and indirect costs (IC). DC considers the cost of purchased equipment (PEC) and operation and maintenance (O&M), whereas IC includes other costs, as shown in Table **3**. The cost of the turbine, pump, condenser, evaporator, and recuperator is included in the equipment investment, as shown in Table **3**. The PEC for ORC equipment shown in Table **2** is calculated as the sum of individual PEC components, with the cost of working fluids disregarded in this study.

2.4.1. Economic Indicators

The economic feasibility of the ORC investment is performed by using a net present value (NPV), levelized cost of electricity, and rate of return on investment. The approach for NPV has been adopted from [11, 40, 41], and is given in Eqn. (14). From Eqn. (14), I_{fuel} and I_{CO2} are the annual income due to fuel and CO_2 savings. The I_{fuel} associates with the energy generated by the ORC which enables a deduction of load on the gas turbine.

Table 3: Assumed parameters for economic modeling [11].

Total Capital Investment (TIC)	I +II
Fixed capital investment (FCI)	DC + IC
Direct cost (DC)	
Purchased equipment costs (PEC)	15% PEC
Purchased equipment installation piping	35% PEC
Instrumentational and controls	12% PEC
Electrical equipment and materials	13% PEC
Indirect cost	
Engineering and supervision	4% DC
Construction costs and contractor’s profit	15% DC
Contingencies	10% of (a &b)
Others cost	
Startup costs	4% FCI
Working capital	15% FCI
Costs of licensing, research, and development	7.5% FCI
Allowance funds used during construction	7.5% FCI

Hence, the saved fuel can be sold to the market subsequently. A reduction of load on natural gas reduces fuel combustion and CO_2 discharge consequently. In that case, CO_2 saving restores the money that could be paid as carbon

$$NPV = \sum_{n=1}^{21} \frac{I_{fuel} + I_{CO2}}{(1+i)^n} - M_f TIC \tag{14}$$

The net present value (NPV) is calculated using the annual income from electricity sales, the cost of CO_2 savings, and the annual expenses. The CO_2 emitted by the gas turbine is calculated using the fuel consumption approach. The CO_2 emissions from the ORC's annual energy generation can be calculated using a conversion factor of 0.0133 $kgCO_2$/kWh, 65 g(fuel)/kWh [41], and an electricity cost of 0.122 US$/kWh in Thailand. *Mf* is set to 0.9 [36]to account for maintenance and operation costs. According to the information provided by Pierobon *et al*. [41], the reasonable amounts for discount rate I and project lifetime (n) are 6% and 20 years, respectively. As shown in Table **3**, the total cost of investment (TIC) includes the cost of components as well as other costs. Table **4** shows cost correlations used to compute the purchasing cost of ORC components.

Table 4: Cost correlations for ORC's components.

Equipment	Cost Correlation	Ref.
Pump	$PEP_p = 378\left[1+\left(\frac{1-0.808}{1-\eta_p}\right)\right]W_p^{0.71}$	[11]
Generator	$PEP_{gen} = 60W_{gen}^{0.95}$	[11]
Turbine	$PEP_T = -16610 + 716W_T^{0.80}$	[11]
Evaporator	$PEC_{eva} = 3650\left(\frac{\dot{q}_{eva}}{\Delta T_{lm,eva}}\right)^{0.8}$	[11]
Condenser	$PEP_C = 30800 + 890A_C^{0.81}$	[11]
Recuperator	$PEC_{rec} = 11256 + 579A^{0.8}$	[42]

The levelized cost of electricity (*LCOE*) is given in Eqn. (15). The total production cost is the sum of the total annual direct cost of manufacturing (C_{DMC}) and fixed cost, as given in Eqn. (16) [8]. The computation of C_{DMC} and C_{FIX} are shown in Table **5**.

$$LCOE = \frac{C_{TIC} + \sum_{t=1}^{21} \frac{C_{TPC}}{(1+i)^t}}{\sum_{t=1}^{21} \frac{M_{el}}{(1+i)^t}} \tag{15}$$

with

$$C_{TPC} = C_{DMC} + C_{FIX} \tag{16}$$

and

$$M_{el} = H_{annual} \times W_{net}^{elec} = 0.9 \times 365 \times 24 \times W_{net}^{elec} \tag{17}$$

where *LCOE* is the levelized cost of electricity (US$/kWh), M_{el} is the annual generated electrical energy (kWh), *i* is the annual discount rate, set 7% [4], *t* is the operational year (*t*=1,2,3,4....). (C_{DMC}) and fixed cost, as given in Eqn. (16) [8]. The computation of C_{DMC} and C_{FIX} are shown in Table **5**.

The rate of return (ROR) is articulated on an annual percentage basis. The net earning is the annual income associated with the electricity selling divided by the cost of investment (TIC) and multiplied by 100 as given in Eqn. (18)

$$ROR = \frac{net\ earning}{C_{TIC}} \tag{18}$$

Table 5: Computation of direct manufacturing and fixed costs [8].

Particular	Description	Formula
Direct cost	Direct manufacturing cost	C_{DMC}
Utilities	Cooling water	14.8 US$/1000m^3
Maintenance	Wages and benefits	C_{WB} = 3.5% C_{TDC}
	Salaries and benefits	C_{SB} = 25% C_{WB}
	Materials and services	C_{MS} = C_{WB}
	Maintenance overhead	C_{MO} = 5%C_{WB}
Fixed costs	Fixed manufacturing costs	C_{FIX}
Property taxes and insurance	Cost of property taxes and liability insurance	C_{PI} = 2% C_{TDC}

3. Equipment and Parameters

When analyzing the performance of ORC systems, the waste heat input required to produce the power output at different heat source temperatures is the most important factor to consider. The flue gas from the SIEMENS SGT-400 gas turbine is used in this study to generate the waste heat. Table **6** shows the design specifications of the gas turbine. Under different expander inlet temperatures, expander inlet pressure, condensation temperature, and different working fluids, the thermodynamic and economic performances of BORC and RORC are compared at 280 °C and 500 °C. To achieve a good match between heat source and heat sink temperatures and cycle boundary conditions, the critical temperature of the working fluid is essential for the selection of working fluids for the recovery of 280-500 °C flue gas.

Table 6: Design specification of gas turbine SGT 400 [43].

Particular	Description
Model	SIEMENS SGT-400
Gross power output	10.5 MWe
Gross efficiency	35.4%
Exhaust gas temperature	510 °C
Exhaust gas mass flowrate	34.2 kg/s
Gross heat rate	10,173 kJ/kWh
Fuel	Natural gas, liquid fuel, dual-fuel

The performance of BORC and RORC was studied in terms of technical and economic. The technical indicators include thermal efficiency and net power output whereas economic indicators include net present value (NPV), rate of return (ROR), and levelized cost of electricity (LCOE). To complete the cost analysis in economic analysis the summary of assumed parameters is listened in Table **7**.

Table 7: Summary of the assumed parameters for cost-benefit analysis.

Parameters	Symbol	Unit	Value	Ref.
Interest rate	*i*	%	6	[2]
Operation and maintenance cost(non- dimension factor)	M_f	-	-	[13]
Life time of investment	*n*	year	20	[2]
Depreciation period	-	year	10	-
Price of fuel (natural gas)	-	US$/kg	0.678	-
Unit cost of electricity	-	US$/kWh	0.122	-
Operating time	op	hrs	8760	[13]

3.1. Validation

For validation, the performance of BORC is compared with those obtained in the literature. Despite numerous studies on the performance of various working fluids, there have been few studies on the performance of the BORC with 200 to 400 kW operating on Toluene or Benzene. Preliminary BORC results obtained by Dai *et al*. [44] and Rashwan *et al*. [38] are used to validate the findings of this study. The two studies employed Ammonia as a working fluid in the BORC. The thermodynamic properties of ammonia and other operating parameters used during the validation of their works are listed in Table **8**.

Table 8: Summary of the input parameters used for validation from literature.

Input Parameter	Dai *et al*. [44]	Rashwan *et al*. [38]	Present Study
Working fluid	Ammonia	Ammonia	Ammonia
Heat source temperature	145 °C	460 °C	400 °C
Amount of heat input	1274 kW	10 MW	-
Expander inlet temperature	135 °C	200 °C	280°C
Expander inlet pressure	3900 kPa	3900 kPa	3600 kPa
Condenser temperature	25 °C	40 °C	40 °C
Condenser pressure	1003 kPa	1369 kPa	1369 kPa
Ambient temperature	20°C	25°C	25°C

The net power output is regarded as an important parameter for validating our study, and it is compared to the literature studied by Dai *et al*. [44] and Rashwan *et al*. [38]. Fig. (**2**) shows a comparison of the net power output in kW versus the expander inlet pressure in the bar. According to the results of the present study, the net power output has a reasonable shape and the values are consistent with those of previous studies concerning the cycle's maximum pressure. The present study-Rashwan *et al.* [38]-and the present study Dai *et al.* [44] show about 4% and 7% deviations at the peak of net power output, respectively. The observed deviations can be attributed to differences in the input parameters such as heat source temperature, heat input, expander inlet temperature, and pressure, as well as assumed parameters such as pump and expander efficiencies, and condensation temperature. Thermal efficiency and net power output, as shown in Table **9**, are in good agreement with Dai *et al*.

[44] and Rashwan *et al*. [38]. As a result of the good agreement between the present study and the literature, the proposed configuration is a solid choice for further investigation.

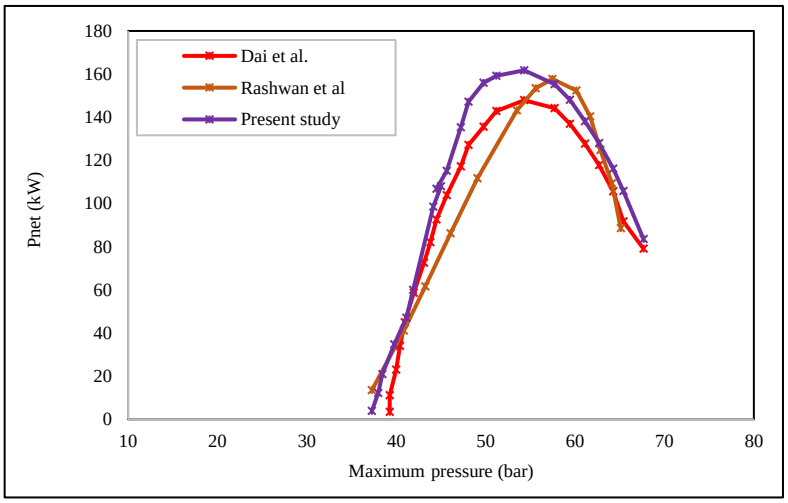

Figure 2: Comparison of the present study with previous studies by Dai *et al*. [44] and Rashwan *et al*. [38].

Table 9: A summary of the comparison between the present study and results from Dai *et al*. [44] and Rashwan *et al*. [38] when ammonia is used as the working fluid.

Input Parameter	Dai *et al*. [44]	Rashwan *et al*. [38]	Present Study
Ammonia mass flow rate (kg/s)	0.931	0.931	0.931
Thermal efficiency (%)	12.10	12.17	12.28
Peak net power output (kW)	147.90	157.883	161.781

4. Results and Discussion

4.1. Effect of Expander Inlet Temperature

Fig. (**3a-b**) shows the effect of expander inlet temperature on net power output and thermal efficiency for BORC and RORC configurationss operating in toluene and benzene, respectively. The expander inlet temperature considered in this study ranges from 530 to 850 K, with the expander inlet pressure remaining constant at 3600 kPa. Fig. (**3a**) depicts a similar trend of net power output (P_{net}) of the BORC when operated with toluene and benzene. At lower expander inlet temperatures of up to 580 K the surge in P_{net} is observed, which is attributed to the high capability of the working fluid to absorb more flue gas's energy. The P_{net} of the BORC increases steadily as the expander inlet temperature rises. Toluene performed well on P_{net}, reaching a maximum value of 349.48 kW at 850 K. At the same temperature of 850 K, benzene achieved a maximum P_{net} of 339.84 kW. In the RORC system, a similar trend of increasing P_{net} with inlet expander temperature is shown in Fig. (**3b**). Due to the effectiveness of the recuperator, a sharp increase is observed at lower expander inlet temperatures of up to 610 K, gradual rise up to 850 followed by a K. With toluene as the working fluid, the RORC achieved a maximum P_{net} of about 349.45 kW. The maximum P_{net} of RORC with benzene was 339.81 kW at an expander inlet temperature of 850 K. Overall, BORC had the highest P_{net} compared to RORC because BORC gained more input heat than RORC while exhibiting more irreversibility. However, the good performance of toluene, as demonstrated in both ORC systems, was also reported in [45] and claimed to be an energy-efficient fluid for heat sources with temperatures above 350 °C. The effect of the expander inlet temperature on the thermal efficiency (η_{th}) of the BORC and RORC is depicted in Fig. (**3a-b**). When the expander inlet temperature rises, η_{th} in BORC rises sharply to the peak and then gradually falls until the expander inlet temperature reaches its maximum. At the expander inlet temperature of about 610 K, the

BORC achieved the highest η_{th} of 27.06% and 26.89 % when operated with toluene and benzene, respectively. For a given expander inlet temperature, η_{th} is similarly increased and then decreased until the expander inlet temperature reaches its maximum. At the expander inlet temperature of 580 K, the maximum η_{th} of the RORC reached 33.30 % and 32.44 %, respectively. When compared to BORC, RORC has the highest η_{th} in both working fluids. Toluene and benzene have increased in η_{th} by approximately 17.12 and 17.10 %, respectively. The increase in η_{th} in RORC is due to the addition of a recuperator, which can use the remaining heat after the turbine to pre-heat the working fluid before the evaporator [44]. In other words, RORC has a higher thermal efficiency than BORC because its average temperature of heat transfer is higher, but its average temperature of heat transfer to the environment is lower.

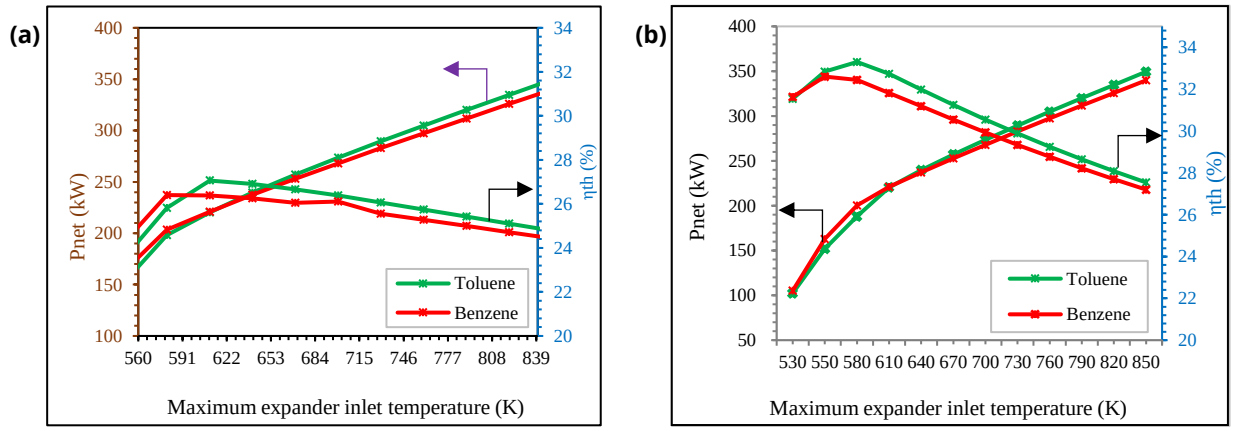

Figure 3: Effect of expander inlet temperature in (**a**) BORC and (**b**) RORC.

Increasing the expander inlet temperature raises the P_{net} of BORC and RORC, with the maximum P_{net} observed at the peak temperature. Because of more heat added to the working fluid, BORC achieved higher power with toluene. In contrast, increasing the expander inlet temperature results in a tiny increase in η_{th}, especially at lower temperatures, while further increasing the temperature results in a gradual fall in η_{th}. As a result, the addition of the recuperator could not significantly improve the performance of the ORCs for waste heat recovery.

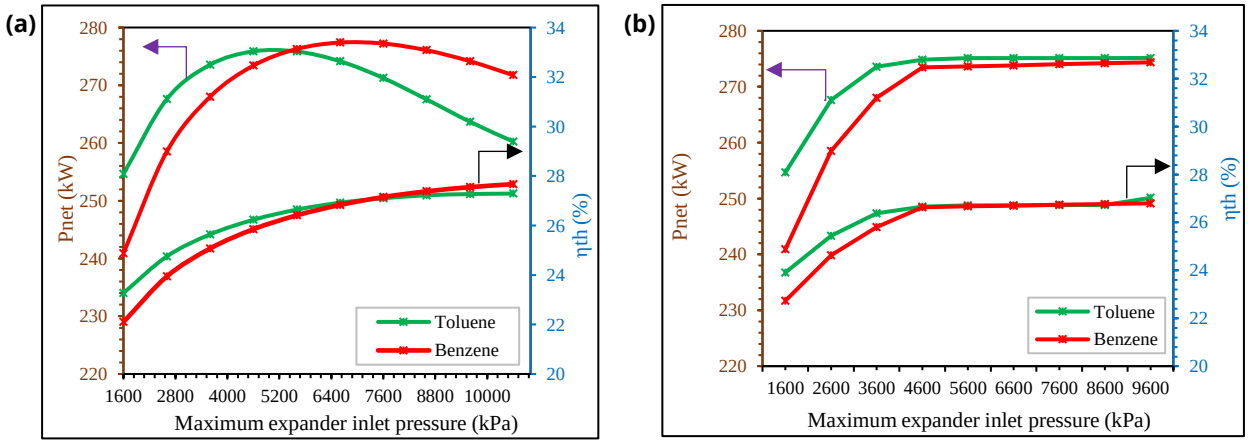

Figure 4: Effect of expander inlet pressure on the P_{net} and η_{th} in (**a**) BORC and (**b**) RORC.

4.2. Effect of Expander Inlet Pressure

The effect of expander inlet pressure on P_{net} and thermal efficiency for BORC and RORC configurations operating in toluene and benzene, respectively as presented in Fig. (**4a-b**). This section varied the expander's inlet pressure from 1600 to 9600 kPa, while keeping the expander's inlet temperature constant at 700 K. Fig. (**4a**)

portrays a similar trend of the BORC's P_{net} when operated with toluene and benzene. At expander inlet pressures of up to 4000 kPa, a sharp increase in P_{net} is observed, which then maintains the profile of both working fluids. As a result, at this stage, *the* P_{net} of the BORC slightly increases as the expander inlet pressure increases. This is because increasing the expander inlet pressure increases the enthalpy difference on the expander, which contributes to a small increase in P_{net}. On P_{net}, toluene performed well, reaching a maximum value of 275.14 kW at 9600 kPa. Similarly to benzene, it achieves a maximum P_{net} of 274.36 kW. In the RORC system, Fig. (**3b**), a similar pattern of increasing P_{net} with inlet expander pressure is depicted. A maximum P_{net} of approximately 271.74 kW was achieved with toluene as the working fluid. With benzene, RORC's maximum P_{net} was 260.27 kW at an expander inlet pressure of 9600 kPa. Finally, BORC experienced the highest P_{net} compared to RORC.

The effect of the expander inlet pressure on the η_{th} of the BORC and RORC is shown in Fig. (**4a-b**), respectively. The η_{th} in BORC increases with expander inlet pressure up to 4600 kPa, and then gradually decreases until the expander inlet temperature reaches its maximum. When the inlet pressure reaches 9600 kPa, the η_{th} of toluene and benzene is 27.03 and 26.8%, respectively. Maximum η_{th} of the RORC reached 33.1 and 33.22 %, respectively, at the expander inlet pressure of 9600 K. For a given expander inlet pressure, η_{th} is similarly increased and then decreased because the pump's power consumption increases, causing η_{th} to decrease consequently [38]. Compared to BORC, RORC has a higher η_{th} in both working fluids. Toluene and benzene have increased in η_{th} by approximately 18.33 and 19.32 %, respectively.

In summary, increasing the expander inlet pressure reduces the P_{net} and η_{th} of BORC and RORC. Despite the drop, BORC had the highest P_{net}, while RORC had the highest η_{th}. Aside from η_{th} enhancement, Ventura and Rowlands [33] reported that there is a threshold point at which a recuperated ORC with any fluid could not have a positive enhancement. To recover waste heat energy, varying the expander inlet pressure is not a viable option because P_{net} drops dramatically when compared to varying the expander inlet temperature.

4.3. Effect of Condensation Temperature

Fig. (**5a-b**) presents the effect of condensation temperature on P_{net} and η_{th} of the BORC and RORC with toluene and benzene used as a working fluid. This section varied the condensation temperature from 20 to 42 °C with an increment of 2°C, while keeping the heat source, the expander's inlet temperature, and pressure are kept constant at 400°C, 700 K to 3600 kPa, respectively. However, in most cases, to reach maximum η_{th} the operating condensation temperature for ORC should range between 15°C to 20°C [46]. As observed in Fig. (**5a-b**), the maximum P_{net} and η_{th} are depicted at the lowest condensation temperature. Beyond 20°C both P_{net} and η_{th} drop monotonically in both BORC and RORC. Consequently, these falls happen since the ambient temperature is higher than the onset condensation temperature, finally, the working fluids can be fully cooled down to achieve higher power output. Therefore, it is recommended that the condensation temperature should not fall below onset if the ambient temperature is lower.

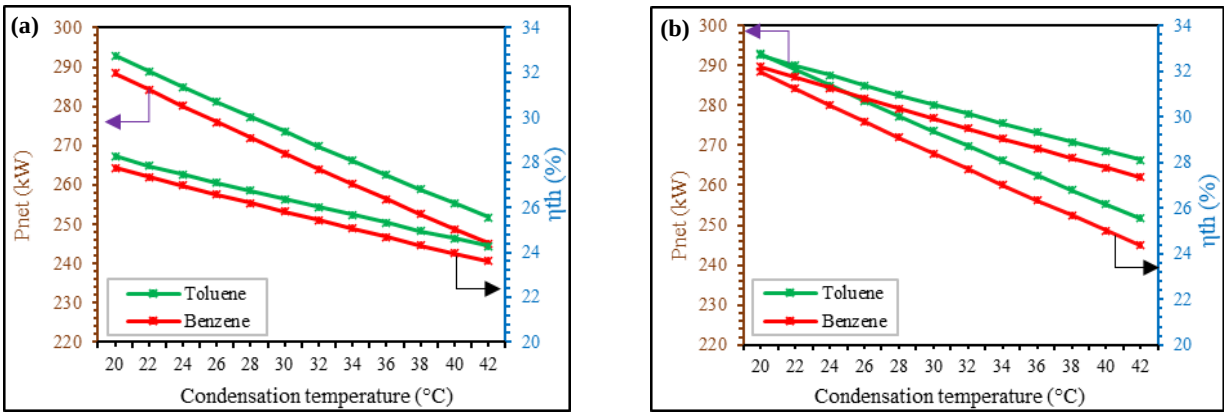

Figure 5: Effect of condensation temperature in (**a**) BORC and (**b**) RORC.

4.4. Effect of Evaporation Temperature

The effect of evaporation temperature on P_{net} and η_{th} for BORC and RORC configurations operating in toluene and benzene, respectively as shown in Fig. (**6a-b**). The evaporation temperature is varied from 280 to 500 °C while maintaining the expander's inlet temperature and pressure constant at 427 °C and 3600 kPa, respectively. When the evaporation temperature rises, the P_{net} of BORC and RORC rise sharply to 320 and 340 °C, respectively, followed by a gradual rise until the evaporation temperature reaches its maximum. The changing trend of P_{net} is caused by an increase in turbine inlet temperature and a decrease in working fluid mass flow as evaporation temperature rises [47, 48]. Toluene performs well on BORC and RORC P_{net} at the highest evaporation temperature of 500 °C, achieving maximum values of 321.77 and 349.45 kW, respectively. Furthermore, as the evaporation temperature rises, the η_{th} of BORC and RORC rise sharply up to 360 °C and then fall for both toluene and benzene fluid. Toluene, on the other hand, has the highest η_{th} of 24.76 and 26.01 % of BORC and RORC configurations, respectively, because η_{th} and inlet enthalpy of the evaporator are proportional. Because of the gradual increase in the evaporator's inlet enthalpy, η_{th} eventually reaches a fixed value for both configurations.

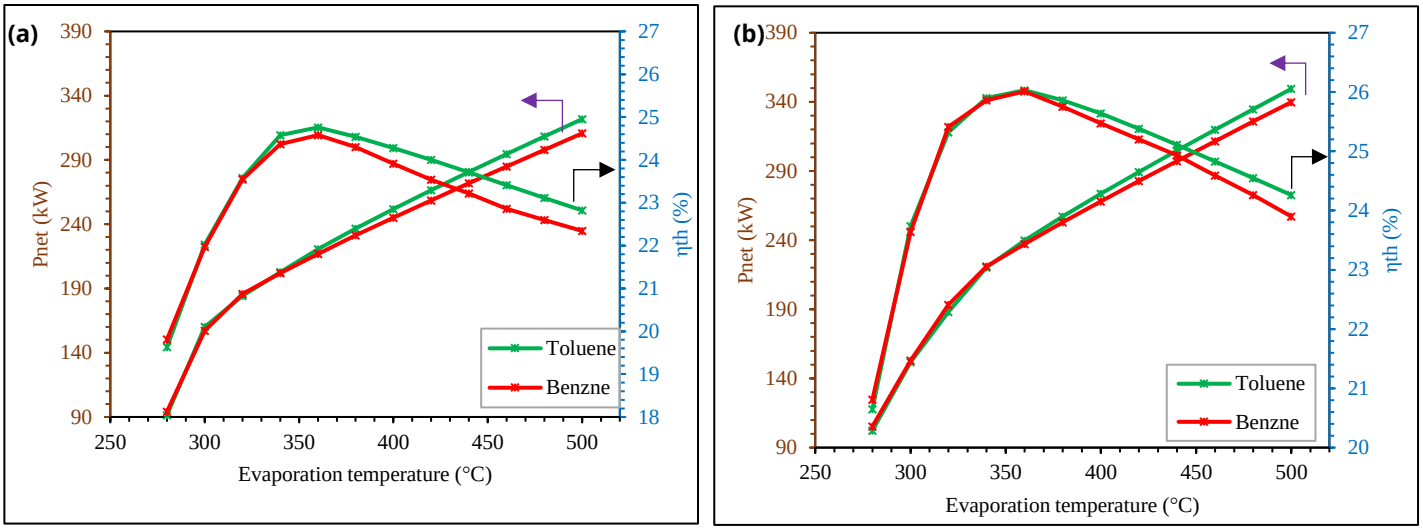

Figure 6: The effect of evaporation temperature on P_{net} and η_{th} of (**a**) BORC and (**b**) RORC systems using toluene and benzene as working fluids.

4.5. Net Present Value

The net present value (NPV) of BORC and RORC as a function of expander inlet temperature is shown in Fig. (**7a-b**), expander inlet pressure in Fig. (**7c-d**), and condensation temperature in Fig. (**7e-f**). The NPVs in Fig. (**7a, c, e**) were observed when the BORC and RORC were operated with toluene, whereas Fig. (**7b, d**) and (**f**) were observed when the BORC and RORC were operated with benzene. It is observed that when the expander inlet temperature is varied, the higher P_{net} results in a greater NPV (Fig. **7a-b**). Furthermore, because of the higher P_{net}, BORC achieves a higher NPV than RORC (Fig. **7a**). BORC has a higher NPV because it captures more heat energy from exhaust flue gas and converts it into useful energy while having a low total investment cost (TIC). Reis *et al*. [35] reported a similar result of higher NPV when BORC was operated with toluene as the working fluid. When compared to benzene, toluene demonstrated a higher NPV with BORC, whereas benzene demonstrated an early turn toward positive NPV. Toluene and benzene achieved maximum NPVs of approximately US$ 815,483.17 and US$ 685,132.40, respectively, at P_n of approximately 349 kW and 340 kW. From Fig. (**7a-b**), it is clear that the NPV for the lifetime of 20 years is slightly higher at 730 K and 820 K for BORC and RORC, respectively, with toluene. The NPV of BORC and RORC in the case of benzene begins to increase at a temperature of 730 K. As a result, the most suitable temperature range for the expander inlet is 730 to 820 K.

The NPV as a function of P_{net} effectuated by the variation in the expander inlet pressure is shown in Fig. (**7c-d**). When affected by expander inlet pressure, both BORC and RORC appear to struggle to achieve higher NPVs. Due

to an increase in the expander's inlet pressure, the enthalpy difference on the expander increases, resulting in a slight increase in P_{net}. Consequently, because of the low P_{net}, BORC, and RORC both struggled to achieve high NPVs, regardless of the working fluid used (Fig. **7c-d**). Therefore, for BORC and RORC with heat sources of up to 673 K and operated with toluene and benzene, varying the expander inlet pressure from 1600 to 9600 kPa would be unnecessary because it would have no benefit on the NPVs.

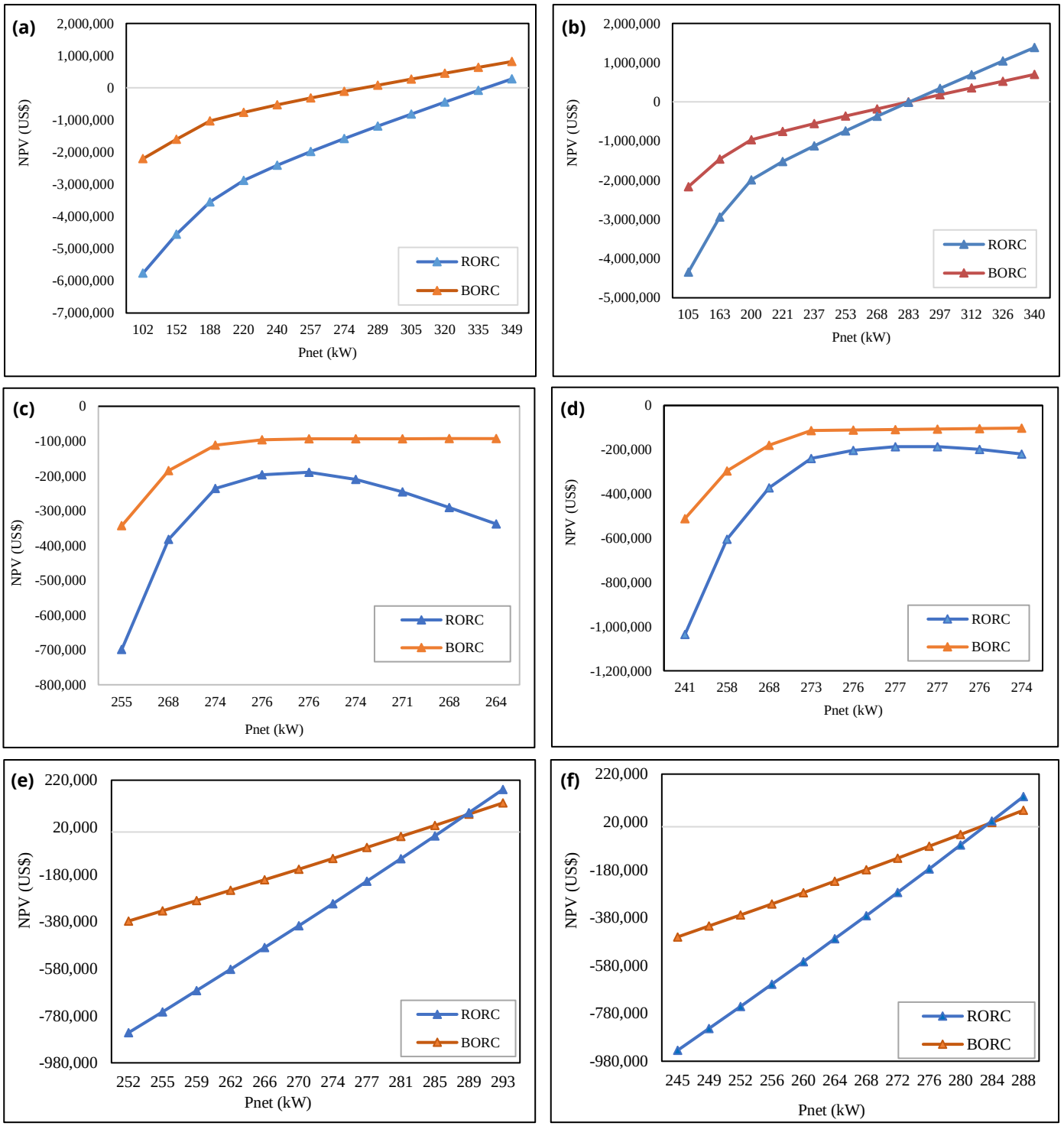

Figure 7: Net present value of BORC and RORC as a function of P_{net} when operated with (**a**, **c**, **e**) toluene and (**b**, **d**, **f**) benzene.

Fig. (**7e-f**) depicts the variation of NPV as a function of Pnet under the influence of condensation temperature. The evaporation temperature of toluene and benzene was set at 500 °C. The condensation temperature ranged

from 20 to 42 °C. The condensation temperature has a significant impact on the NPV of BORC and RORC. It was discovered that at a lower condensation temperature of 20 °C, a higher P_{net} was produced because the working fluid temperature dropped rapidly and absorbed more heat energy from the heat source. Consequently, the higher P_{net} resulted in higher NPVs. In Fig. (**7e-f**), the NPV is shown to increase monotonically as P_{net} increases. It is obvious that at a condensation temperature of 20 °C, in Fig. (**7e-f**), toluene could achieve a maximum P_{net} of 293 kW, resulting in NPVs of approximately US$ 123,658.66 in BORC and US$ 111,911.61 in RORC. Furthermore, when compared to RORC and other working fluids, BORC quickly achieves positive NPV with toluene as the working fluid. As a result, for waste heat recovery, a lower condensation temperature would result in higher P_{net} and NPV. But for temperatures below 15 °C, the working fluid will be further cooled after condensation, which will cause a delay in phase charging after the evaporator. The condenser will also be larger and more expensive, which will reduce ORC system performance as well as its efficiency and effectiveness. To obtain a condensation temperature below 15 °C, however, a cooling medium with a temperature of 5-7 °C is required, which is not readily available in most hot countries. This necessitates the purchase of additional equipment, such as a chiller, which has financial implications.

4.6. Rate of Return

The rate of return (ROR) of BORC and RORC as a function of expander inlet temperature is shown in Fig. (**8a-b**), expander inlet pressure in Fig. (**8c-d**), and condensation temperature in Fig. (**8e-f**). The RORs in Fig. (**8a**, **c**, **e**) were observed when the BORC and RORC were operated with toluene, whereas Fig. (**8b, d**) and (**f**) were observed when the BORC and RORC were operated with benzene. In Fig. (**8a-b**), it can be seen that ROR increases exponentially as P_{net} increases. BORC and RORC achieved a maximum ROR of about 26.11 % with toluene at a maximum P_{net} of 349.45 kW. When used with benzene as the working fluid, BORC and RORC achieved a maximum ROR of 25.39 %. Furthermore, toluene performed well in terms of ROR, achieving the highest ROR of 26.11 % at the maximum expander inlet temperature of 850 K, which is 2.76 % higher than benzene.

Fig. (**8c-d**) illustrates the variation ROR as a function of P_{net} under the influence of expander inlet pressure. In the case of toluene, increasing P_{net} causes ROR to rise to 20.61 % and then remain constant until P_{net} reaches its maximum. In contrast, ROR increases with P_{net} up to 20.76 % for benzene and then gradually decreases until P_{net} reaches its maximum. It is worth noting that the highest ROR of approximately 20.79 % was obtained with BORC operated with benzene at 277 kW, which corresponds to an expander inlet pressure of 7600 kPa. Fig. (**8e-f**) shows the ROR as a function of P_{net} under the impact of condensation temperature. It can be seen from Fig. (**8e**) that with the increase of P_{net}, ROR increases proportionally. It is evident that with BORC, the maximum ROR reached approximately 21.96 and 21.62 % for toluene and benzene, respectively. However, the numerical values are very similar for the two working fluids i.e., Toluene and benzene since the molecular weights of the two working fluids are very close while the results show that when the P_{net} of BORC is 292.87 and 288.37 kW, the difference in ROR when operated with toluene and benzene is 0.34%, indicating that BORC with toluene has a higher ROR than with benzene.

4.7. Levelized Cost of Electricity

The levelized cost of electricity (LCOE) of BORC and RORC as a function of P_{net} influence by expander inlet temperature is shown in Fig. (**9a-b**), expander inlet pressure in Fig. (**9c-d**), and condensation temperature in Fig. (**9e-f**). The LCOEs in Fig. (**9a**, **c**, **e**) were observed when the BORC and RORC operated with toluene, whereas Fig. (**9b**, **d**, and **f**) were observed when the BORC and RORC operated with benzene. The LCOE sharply drops as P_{net} increases from 102 to 220 kW in toluene and 105 to 221 kW in benzene, as shown in Fig. (**9a-b**). Subsequently, the LCOE gradually declines until it reaches its maximum. At P_{net} of 349 kW, RORC and BORC had the lowest LCOE approximately 0.0534 US$/kWh and 0.0532 US$/kWh, respectively, when operating on toluene. In contrast, with benzene had the lowest LCOE of 0.0547 US$/kWh and 0.0549 US$/kWh at P_{net} of about 340 kW, respectively. With these results, it is worth noting that the BORC with toluene has the lowest LCOE of 0.0532 US$/kWh at a P_{net} of 349 kW and an expander inlet temperature of 850 K.

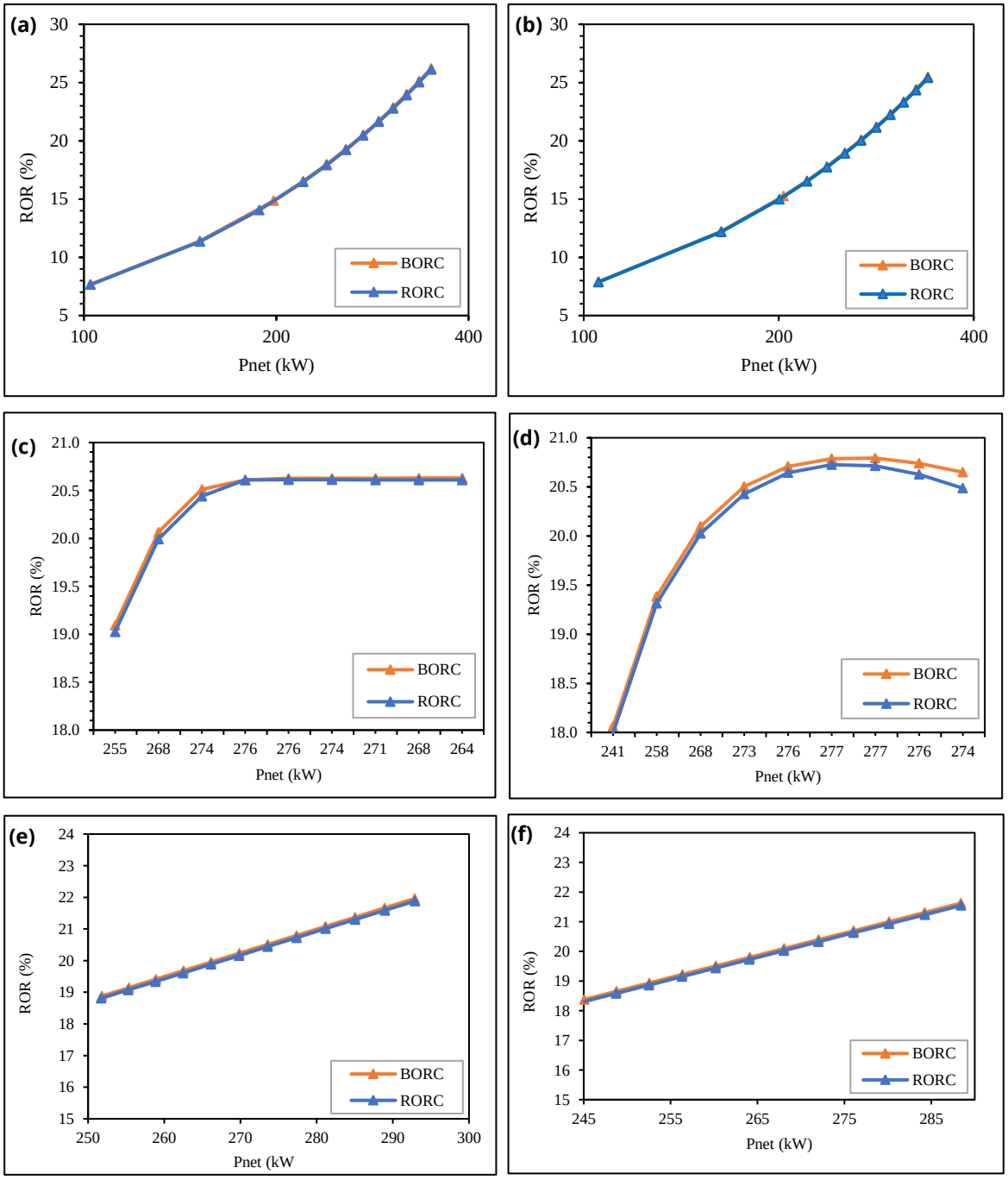

Figure 8: Rate of return (ROR) of BORC and RORC as a function of P_{net} when operated with (**a**, **c**, **e**) toluene and (**b**, **d**, **f**) benzene.

Under the influence of expander inlet pressure, LCOE reaches the lowest values of 0.0676 US$/kWh at *a* P_{net} of 263.7 kW in both RORC and BORC operated with toluene. In contrast, RORC and BORC with benzene had the lowest LCOE of 0.0673 US$/kWh at *a* P_{net} of about 277.4 kW, respectively. The effective expander inlet pressure required to achieve the lowest LCOE in toluene and benzene is approximately 9600 kPa.

When influenced by the condensation temperature, LCOE falls drastically with the increased P_{net} and attains the lowest value of 0.0635 US$/kWh at Pnet of 292.87 kW in BORC with toluene and condensation temperature of 20 °C. As the condensation temperature dropped, the ORC's Pnet increased. As a result, the RORC achieved a higher P_{net} of 292.90 kW with toluene than in BORC. Despite having a higher P_{net}, the LCOE of RORC with toluene was higher (0.0637411 US$/kWh) than that of BORC (0.0635 US$/kWh). This is because RORC has a higher

equipment cost than BORC. To demonstrate the risky practice of bottom-up cost estimation for ORC plants, this paper compares BORC and RORC start-up costs from the literature with costs obtained from a rough bottom-up estimate. The research focuses on ORC for waste heat recovery.

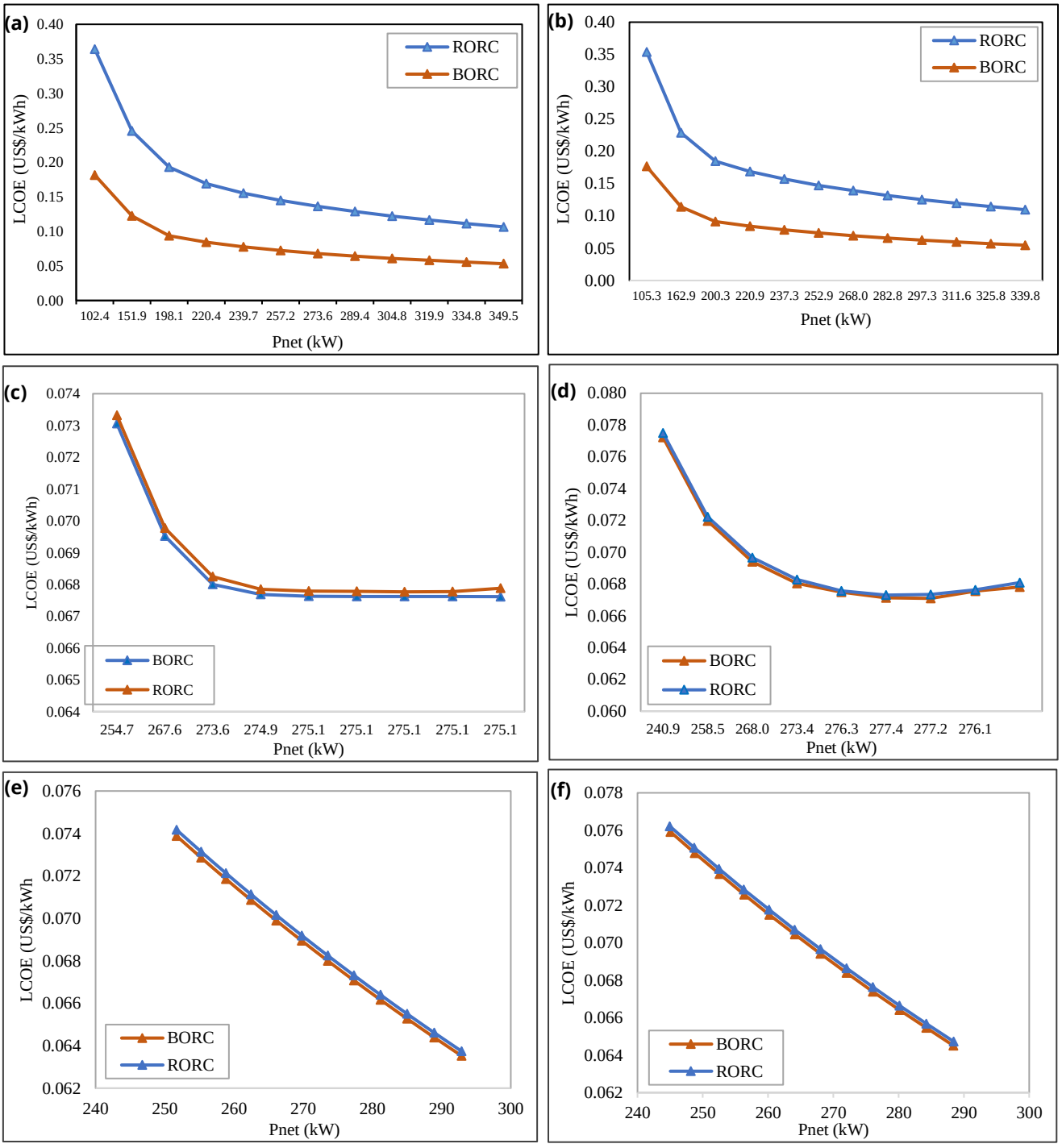

Figure 9: Levelized cost of electricity (LCOE) of BORC and RORC as a function of P_{net} when operated with (**a**, **c**, **e**) toluene and (**b**, **d**, **f**) benzene.

The heat source is a low-medium temperature (150-250°C) gas turbine flue gas stream. The ORC system was integrated into the plant by utilizing an intermediate of two selected working fluids, namely Toluene and Benzene, as well as a flue gas heat exchanger. A centrifugal pump, expander, and generator comprise the ORC system. Condensation occurs in an air-cooled evaporator, which is a plate heat exchanger. The estimated initial cost of

investment for BORC and RORC are presented in Fig. (**10**). The BORC costs about US$ 74, 578.63 which is 0.35% lower than the RORC. The higher cost of the RORC is due to the addition of a recuperator. The estimation of the purchased cost of the equipment was based on 400 kW. ORC. As shown in Fig. (**10**) the most expensive equipment are Evaporator and condenser. In BORC the total equipment cost as in the RORC evaporator accounts for 45.54%. These cost proportions are in line with those estimated in [31, 49].

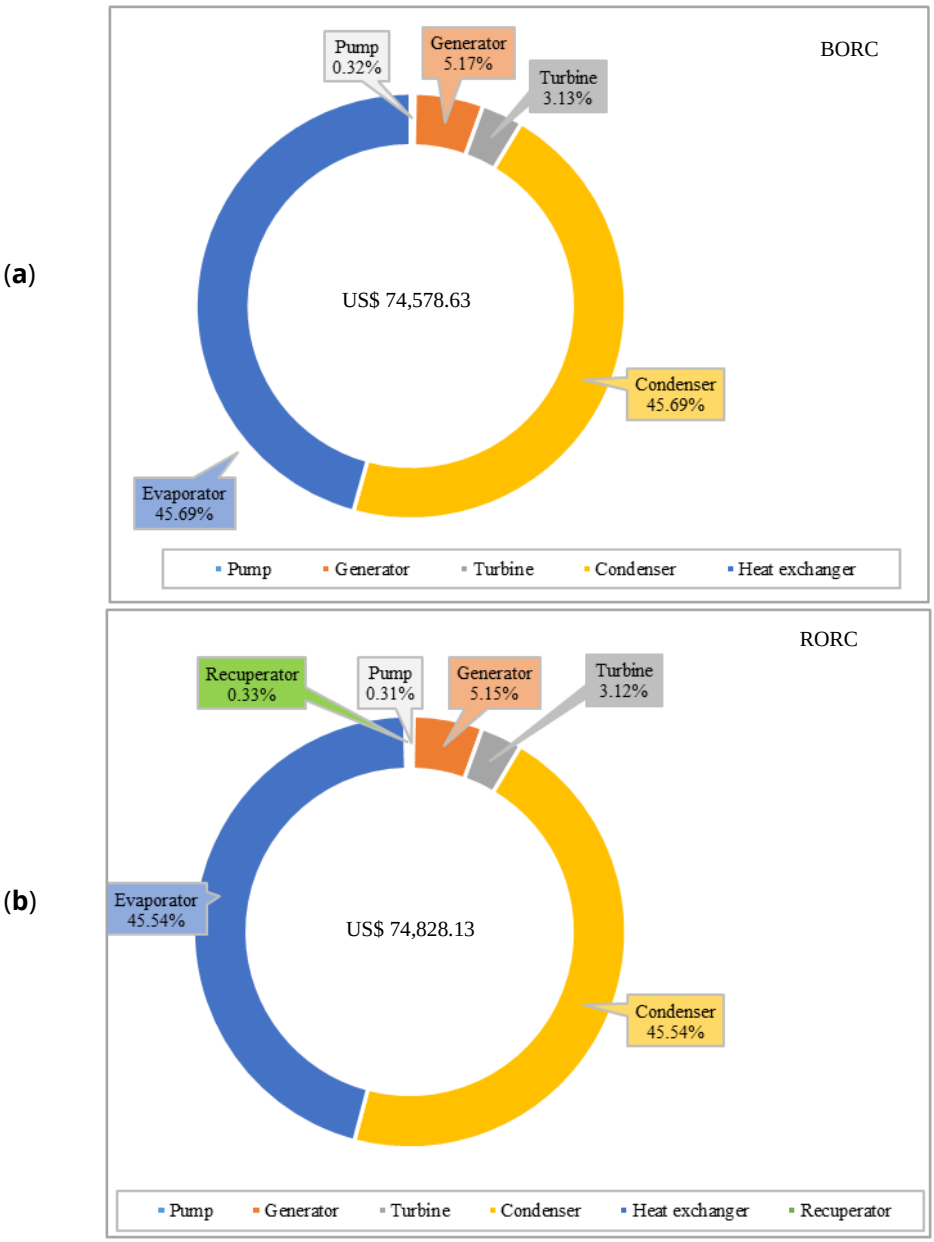

Figure 10: The breakdown of initial investment cost of (**a**) BORC and (**b**) RORC.

5. Conclusion

To better understand the performance of the organic Rankine cycle (ORC) for waste heat to power generation, a basic ORC (BORC) and an ORC with recuperator (RORC) with two different heat sources and working fluids are investigated. Operational effects, such as expander inlet temperature, expander inlet pressure, evaporation temperature, and condensation temperature, were used to examine the performance of the ORCs and determine the best working conditions from both a thermodynamic and an economic standpoint. Technical performance consists of net power output and thermal efficiency, while economic analysis consists of net present value (NPV), rate of return on investment (ROR), and levelized cost of electricity (LCOE). The following are the main conclusions:

- From a thermodynamic standpoint, the BORC can convert more waste heat to useful energy to increase net power output, but at the expense of thermal efficiency. Increasing the expander inlet temperature and pressure could significantly improve the BORC's net power over the RORC. Furthermore, evaporation temperature increases the net power output proportionally, whereas condensation temperature decreases the net power output of the ORCs.
- A better thermal efficiency is achieved by RORC than BORC. Increasing the expander inlet temperature and pressure could not appreciably enhance the thermal efficiency of ORCs. Despite of little improvement, RORC achieved higher thermal efficiency than the BORC one. Likewise, evaporation and condensation temperatures showed a slight improvement in thermal efficiency.
- In terms of economics, heat source has a significant impact on the net present value of BORC and RORC. The high NPV is due to higher net power output, which is influenced by expander inlet temperature and pressure.
- The rate of return on investment of both BORC and RORC improves exponentially with an increase in expander inlet temperature and slightly improves with an increase in expander inlet pressure and condensation temperature.
- The lowest LCOE of 0.0532 US$/kWh is from BORC operated with toluene at a net power output of 349 kW and decreases with an increase in expander inlet temperature.
- Toluene performed better with BORC in net power output, quickly achieved positive net present value, attained a higher rate of return, and the lowest levelized cost of electricity.
- The additional of recuperator adds the costs of initial investment and levelized cost of electricity of the system and does not improve the performance of the ORCs for waste heat recovery.

Nomenclature

$\Delta T_{lm,eva}$	Temperature pinch difference	m	Mass flow rate
A	Area (m^2)	Mel	Annual generated electricity
BORC	Basic organic rankine cycle	NPV	Net present value
C_{DMC}	Direct manufacturing cost	ODP	Ozone depletion potential
C_{FIX}	Fixed cost	ORC	Organic rankine cycle
CP	Specific heat capacity (kJ/kg K)	PEP	Purchase equipment cost
CPI	Cost of property taxes and liability insurance	P_{net}	Net present value
C_{TPC}	Total purchasing cost	PPTD	Pinch point temperature difference
cw	Cooling water	*Q*	Amount of heat flow rate (kW)
DC	Direct cost	q_{eva}	Heat rate in the evaporator
EXP	Expander	ROR	Rate of return
FCI	Fixed capita investment	RORC	Recuperator organic rankine cycle
GT	Gas turbine	*s*	Entropy (kg/kJ. K)
GWP	Global worming potential	*T*	Temperature
h	Specific enthalpy (kg/kJ)	TCI	Total cost of investment
i	Interest rate	*W*--	Power
IC	Indirect cost	W_p	Pump work
K	Kelvin	W_T	Turbine work
LCOE	Levalized cost of electricity		

Subscript

c	condenser
e	evaporator
ext,g	exhaust gas
ext,in	exhaust in
g	generator
in	inlet of each point
net	net
out	outlet of each point
p	pump
t	turbine
wf	working fluid

Greek symbols

η_{th}	Thermal efficiency

Conflict of Interest

The authors declare no conflict of interest.

Funding

The study received no financial support.

Acknowledgments

The authors would like to express their gratitude to The Dar es Salaam Institute of Technology. This paper does not necessarily reflect the views of supporters.

References

[1] Basta G, Meloni N, Poli F, Talluri L, Manfrida G. Energy, exergy and exergo-economic analysis of an OTEC power plant utilizing kalina cycle. Glob J Energ Technol Res Updat. 2021; 8: 1-18. https://doi.org/10.15377/2409-5818.2021.08.1

[2] Wang J, Wang J, Dai Y, Zhao P. Thermodynamic analysis and optimization of a transcritical CO2 geothermal power generation system based on the cold energy utilization of LNG. Appl Therm Eng. 2014; 70: 531-40. https://doi.org/10.1016/j.applthermaleng.2014.05.084

[3] Greyson KA, Gerutu GB, Bobi S, Chombo PV. Exploring the potential of compressed natural gas as a sustainable fuel for rickshaw: A case study of Dar es Salaam. J Nat Gas Sci Eng. 2021; 96: 104273. https://doi.org/10.1016/j.jngse.2021.104273

[4] Gerutu GB, Greyson KA, Chombo PV. Compressed natural gas as an alternative vehicular fuel in tanzania: implementation, barriers, and prospects. Methane. 2023; 2: 66-85. https://doi.org/10.3390/methane2010006

[5] Gerutu G, Mohamed C, Chombo P. Transition to compressed natural gas rickshaws for urban mobility: a case of dar es salaam city. J Logist Manag Eng Sci. 2021; 03: 81-7.

[6] Wang J, Liu W, Liu G, Sun W, Li G, Qiu B. Theoretical design and analysis of the waste heat recovery system of turbine exhaust steam using an absorption heat pump for heating supply. Energies. 2020; 13(23), 6256. https://doi.org/10.3390/en13236256

[7] Zhang A, Zhang H, Qadrdan M, Yang W, Jin X, Wu J. Optimal planning of integrated energy systems for offshore oil extraction and processing platforms. Energies. 2019; 12(4): 756. https://doi.org/10.3390/en12040756

[8] Le VL, Kheiri A, Feidt M, Pelloux-Prayer S. Thermodynamic and economic optimizations of a waste heat to power plant driven by a subcritical ORC (Organic Rankine Cycle) using pure or zeotropic working fluid. Energy. 2014; 78: 622-38. https://doi.org/10.1016/j.energy.2014.10.051

[9] Song J, Loo P, Teo J, Markides CN. Thermo-economic optimization of organic rankine cycle (ORC) systems for geothermal power generation: A comparative study of system configurations. Front Energy Res. 2020; 8: Article 6. https://doi.org/10.3389/fenrg.2020.00006

[10] Yang F, Zhang H, Bei C, Song S, Wang E. Parametric optimization and performance analysis of ORC (organic Rankine cycle) for diesel engine waste heat recovery with a fin-and-tube evaporator. Energy. 2015; 91: 128-41. https://doi.org/10.1016/j.energy.2015.08.034

[11] Habka M, Ajib S. Analytical and comparative study of a mini solar-powered cogeneration unit based on organic rankine cycle for low-temperature applications. Glob J Energy Technol Res Updat. 2014; 1: 40-56. https://doi.org/10.15377/2409-5818.2014.01.01.4

[12] Zhao Y, Du B, Chen S, Zhao J, Gong Y, Bu X, *et al*. Thermo-economic comparison between organic rankine cycle and binary-flashing cycle for geothermal energy. Front Earth Sci (Lausanne). 2021; 9: Article 759872. https://doi.org/10.3389/feart.2021.759872

[13] Basaran A, Ozgener L. Investigation of the effect of different refrigerants on performances of binary geothermal power plants. Energy Convers Manag. 2013; 76: 483-98. https://doi.org/10.1016/j.enconman.2013.07.058

[14] Reis MML, Guillen JA V, Gallo WLR. Off-design performance analysis and optimization of the power production by an organic rankine cycle coupled with a gas turbine in an offshore oil platform. Energy Convers Manag. 2019; 196: 1037-50. https://doi.org/10.1016/j.enconman.2019.06.051

[15] Mahmoudi A, Fazli M, Morad MR. A recent review of waste heat recovery by organic rankine cycle. Appl Therm Eng. 2018; 143: 660-75. https://doi.org/10.1016/j.applthermaleng.2018.07.136

[16] Huang H, Zhu J, Yan B. Comparison of the performance of two different Dual-loop organic Rankine cycles (DORC) with nanofluid for engine waste heat recovery. Energy Convers Manag. 2016; 126: 99-109. https://doi.org/10.1016/j.enconman.2016.07.081

[17] Zarogiannis T, Papadopoulos AI, Seferlis P, Linke P. The impact of novel and conventional working fluids on the control performance in organic rankine cycles. Comput Aided Chem Eng. 2017; 40: 2443-8. https://doi.org/10.1016/B978-0-444-63965-3.50409-8

[18] Zhai H, An Q, Shi L, Lemort V, Quoilin S. Categorization and analysis of heat sources for organic rankine cycle systems. Renew Sustain Energy Rev. 2016; 64: 790-805. https://doi.org/10.1016/j.rser.2016.06.076

[19] Li J, Ge Z, Duan Y, Yang Z. Effects of heat source temperature and mixture composition on the combined superiority of dual-pressure evaporation organic Rankine cycle and zeotropic mixtures. Energy 2019; 174: 436-49. https://doi.org/10.1016/j.energy.2019.02.186

[20] Chauhan A, Vaish R. Fluid selection of organic Rankine cycle using decision making approach. J Comput Eng. 2013; 2013: 1-10. https://doi.org/10.1155/2013/105825

[21] Thurairaja K, Wijewardane A, Jayasekara S, Ranasinghe C. Working fluid selection and performance evaluation of ORC. Energy Procedia. 2019; 156: 244-8. https://doi.org/10.1016/j.egypro.2018.11.136

[22] Wang X, Levy EK, Pan C, Romero CE, Banerjee A, Rubio-Maya C, *et al*. Working fluid selection for organic rankine cycle power generation using hot produced supercritical CO2 from a geothermal reservoir. Appl Therm Eng. 2019; 149: 1287-304. https://doi.org/10.1016/j.applthermaleng.2018.12.112

[23] Motamed MA, Nord LO. Part-load efficiency boost in offshore organic rankine cycles with a cooling water flow rate control strategy. Energy. 2022; 257: 124713. https://doi.org/10.1016/j.energy.2022.124713

[24] Motamed MA, Nord LO. Assessment of organic rankine cycle part-load performance as gas turbine bottoming cycle with variable area nozzle turbine technology. Energies. 2021; 14(23): 7916. https://doi.org/10.3390/en14237916

[25] Wang X, Shu G, Tian H, Feng W, Liu P, Li X. Effect factors of part-load performance for various organic rankine cycles using in engine waste heat recovery. Energy Convers Manag. 2018; 174: 504-15. https://doi.org/10.1016/j.enconman.2018.08.024

[26] Zhang X, Wang X, Cai J, He Z, Tian H, Shu G, *et al*. Experimental study on operating parameters matching characteristic of the organic rankine cycle for engine waste heat recovery. Energy. 2022; 244: 122681. https://doi.org/10.1016/j.energy.2021.122681

[27] Javanshir A, Sarunac N. Thermodynamic analysis of a simple organic rankine cycle. Energy. 2017; 118: 85-96. https://doi.org/10.1016/j.energy.2016.12.019

[28] Yan J, Jia W, Li K, Yu H, Guo X. Energy analysis of cyclic parameters of organic rankine cycle system. Int J Low-Carbon Technol. 2021; 16: 341-50. https://doi.org/10.1093/ijlct/ctaa053

[29] Pierobon L, Larsen U, Van Nguyen T, Haglind F. Optimization of organic rankine cycles for off-shore applications. Proceedings of ASME Turbo Expo 2013: Turbine Technical Conference and Exposition June 3-7, 2013, San Antonio, Texas, USA: ASME; 2013. https://doi.org/10.1115/GT2013-94108

[30] Chacartegui R, Sánchez D, Muñoz JM, Sánchez T. Alternative ORC bottoming cycles for combined cycle power plants. Appl Energy. 2009; 86: 2162-70. https://doi.org/10.1016/j.apenergy.2009.02.016

[31] Liu W, Zhang X, Zhao N, Shu C, Zhang S, Ma Z, *et al*. Performance analysis of organic Rankine cycle power generation system for intercooled cycle gas turbine. Adv Mech Eng. 2018; 10(8): 1-12. https://doi.org/10.1177/1687814018794074

[32] Algieri A, Morrone P. Comparative energetic analysis of high-temperature subcritical and transcritical Organic Rankine Cycle (ORC). A biomass application in the Sibari district. Appl Therm Eng. 2012; 36: 236-44. https://doi.org/10.1016/j.applthermaleng.2011.12.021

[33] de M. Ventura CA, Rowlands AS. Recuperated power cycle analysis model: Investigation and optimisation of low-to-moderate resource temperature Organic Rankine Cycles. Energy. 2015; 93: 484-94. https://doi.org/10.1016/j.energy.2015.09.055

[34] Rahbar K, Mahmoud S, Al-Dadah RK, Moazami N, Mirhadizadeh SA. Review of organic Rankine cycle for small-scale applications. Energy Convers Manag. 2017; 134: 135-55. https://doi.org/10.1016/j.enconman.2016.12.023

[35] Reis MML, Gallo WLR. Study of waste heat recovery potential and optimization of the power production by an organic Rankine cycle in an FPSO unit. Energy Convers Manag. 2018; 157: 409-22. https://doi.org/10.1016/j.enconman.2017.12.015

[36] Valencia G, Fontalvo A, Cárdenas Y, Duarte J, Isaza C. Energy and exergy analysis of different exhaust waste heat recovery systems for natural gas engine based on ORC. Energies. 2019; 12(12): 2378. https://doi.org/10.3390/en12122378

[37] Fontalvo A, Solano J, Pedraza C, Bula A, Gonzalez Quiroga A, Vasquez Padilla R. Energy, exergy and economic evaluation comparison of small-scale single and dual pressure organic Rankine cycles integrated with low-grade heat sources. Entropy. 2017; 19(10): 476. https://doi.org/10.3390/e19100476

[38] Rashwan SS, Dincer I, Mohany A. Analysis and assessment of cascaded closed loop type organic rankine cycle. Energy Convers Manag. 2019; 184: 416-26. https://doi.org/10.1016/j.enconman.2018.12.089

[39] Li T, Meng N, Liu J, Zhu J, Kong X. Thermodynamic and economic evaluation of the organic rankine cycle (ORC) and two-stage series organic Rankine cycle (TSORC) for flue gas heat recovery. Energy Convers Manag. 2019; 183: 816-29. https://doi.org/10.1016/j.enconman.2018.12.094

[40] Pierobon L, Nguyen T-V, Larsen U, Haglind F, Elmegaard B. Multi-objective optimization of organic rankine cycles for waste heat recovery: Application in an offshore platform. Energy. 2013; 58: 538-49. https://doi.org/10.1016/j.energy.2013.05.039

[41] Pierobon L, Benato A, Scolari E, Haglind F, Stoppato A. Waste heat recovery technologies for offshore platforms. Appl Energy. 2014; 136: 228-41. https://doi.org/10.1016/j.apenergy.2014.08.109

[42] Nusiaputra Y, Wiemer H-J, Kuhn D. Thermal-Economic modularization of small, organic Rankine cycle power plants for mid-enthalpy geothermal fields. Energies. 2014; 7: 4221-40. https://doi.org/10.3390/en7074221

[43] SGT-400: Industrial gas turbine. Siemens Energy 2021. https://www.siemens-energy.com/global/en/offerings/power-generation/gas-turbines/sgt-400.html (Accessed on October 26, 2023).

[44] Dai Y, Wang J, Gao L. Parametric optimization and comparative study of organic Rankine cycle (ORC) for low grade waste heat recovery. Energy Convers Manag. 2009; 50: 576-82. https://doi.org/10.1016/j.enconman.2008.10.018

[45] Tian H, Liu L, Shu G, Wei H, Liang X. Theoretical research on working fluid selection for a high-temperature regenerative transcritical dual-loop engine organic Rankine cycle. Energy Convers Manag. 2014; 86: 764-73. https://doi.org/10.1016/j.enconman.2014.05.081

[46] Li J, Pei G, Ji J, Bai X, Li P, Xia L. Design of the ORC (organic Rankine cycle) condensation temperature with respect to the expander characteristics for domestic CHP (combined heat and power) applications. Energy. 2014; 77: 579-90. https://doi.org/10.1016/j.energy.2014.09.039

[47] Kolahi M, Yari M, Mahmoudi SMS, Mohammadkhani F. Thermodynamic and economic performance improvement of ORCs through using zeotropic mixtures: Case of waste heat recovery in an offshore platform. Case Stud Therm Eng. 2016; 8: 51-70. https://doi.org/10.1016/j.csite.2016.05.001

[48] Toffolo A, Lazzaretto A, Manente G, Paci M. A multi-criteria approach for the optimal selection of working fluid and design parameters in Organic Rankine Cycle systems. Appl Energy. 2014; 121: 219-32. https://doi.org/10.1016/j.apenergy.2014.01.089

[49] Song J, Gu C, Ren X. Parametric design and off-design analysis of organic Rankine cycle (ORC) system. Energy Convers Manag. 2016; 112: 157-65. https://doi.org/10.1016/j.enconman.2015.12.085